Faraday Discussions

Accepted Manuscript

This manuscript will be presented and discussed at a forthcoming Faraday Discussion meeting. All delegates can contribute to the discussion which will be included in the final volume.

Register now to attend! Full details of all upcoming meetings: http://rsc.li/fd-upcoming-meetings

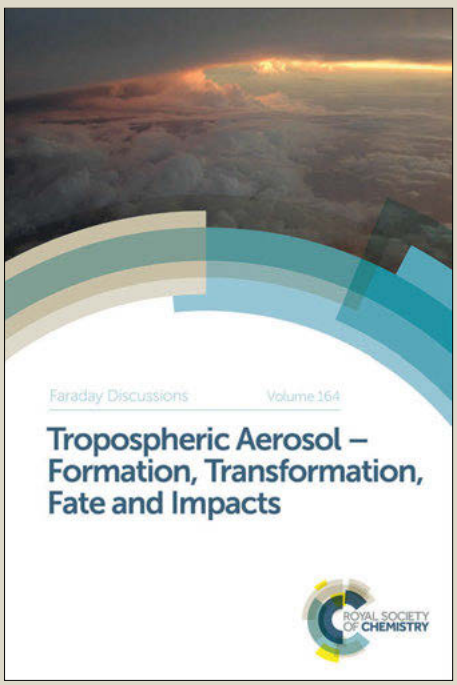

This is an *Accepted Manuscript*, which has been through the Royal Society of Chemistry peer review process and has been accepted for publication.

Accepted Manuscripts are published online shortly after acceptance, before technical editing, formatting and proof reading. Using this free service, authors can make their results available to the community, in citable form, before we publish the edited article. We will replace this *Accepted Manuscript* with the edited and formatted *Advance Article* as soon as it is available.

You can find more information about *Accepted Manuscripts* in the Information for Authors.

Please note that technical editing may introduce minor changes to the text and/or graphics, which may alter content. The journal's standard Terms & Conditions and the Ethical guidelines still apply. In no event shall the Royal Society of Chemistry be held responsible for any errors or omissions in this *Accepted Manuscript* or any consequences arising from the use of any information it contains.

ROYAL SOCIETY OF CHEMISTRY

www.rsc.org/faraday_d

CREATED USING THE RSC LaTeX PCCP ARTICLE TEMPLATE – SEE www.rsc.org/electronicfiles FOR DETAILS
PAPER www. rsc.org/faraday_d | Faraday Discussions

Non-equilibrium Dirac carrier dynamics in graphene investigated with time- and angle-resolved photoemission spectroscopy

Isabella Gierz,*[a] Stefan Link,[b] Ulrich Starke,[b] and Andrea Cavalleri [a]

Received Xth XXXXXXXXXX 20XX, Accepted Xth XXXXXXXXX 20XX
First published on the web Xth XXXXXXXXXX 200X
DOI: 10.1039/c000000x

We have used time- and angle-resolved photoemission spectroscopy (tr-ARPES) to assess the influence of many-body interactions on the Dirac carrier dynamics in graphene. From the energy-dependence of the measured scattering rates we directly determine the imaginary part of the self-energy, visualizing the existence of a relaxation bottleneck associated with electron-phonon coupling. A comparison with static line widths obtained by high-resolution ARPES indicates that the dynamics of photo-excited carriers in graphene are solely determined by the equilibrium self-energy. Furthermore, the subtle interplay of different many-body interactions in graphene may allow for carrier multiplication, where the absorption of a single photon generates more than one electron-hole pair via impact ionization. We find that, after photo-excitation, the number of carriers in the conduction band along the ΓK-direction keeps increasing for about 40 fs after the pump pulse is gone. A definite proof of carrier multiplication in graphene, however, requires a more systematic study, carefully taking into account the contribution of momentum relaxation on the measured rise time.

1 Introduction: quasiparticle dynamics in graphene

The peculiar electronic structure of graphene results from the conical intersection of two cosine-shaped bands at the K-point of the hexagonal Brillouin zone. While the single-particle dispersion is well described by a simple tight-binding model[1], it has been shown that the linear band structure in the vicinity of the Fermi level is strongly renormalized by many-body interactions[2,3]. A careful line width analysis based on high-resolution ARPES measurements has revealed that the photo-hole decays into phonons, electron-hole pairs, and plasmons[2]. The influence of a particular decay channel depends strongly on energy. Decay via phonon emission becomes important for energies $|E| > \hbar\omega_{ph}$, while the emission of plasmons is restricted to the region around the Dirac point E_D, where valence

[a] *Max Planck Institute for the Structure and Dynamics of Matter, Hamburg, Germany.*
[b] *Max Planck Institute for Solid State Research, Stuttgart, Germany.*
* Fax: +49 (0)40 8998 1958; Tel: +49 (0)40 8998 5362; E-mail: isabella.gierz@mpsd.mpg.de

and conduction band touch. Electron-hole pairs dominate the relaxation for energies $|E| > 2E_D$[2]. The decay of photo-excited carriers via many-body interactions can be directly observed in the time domain[4].

From previous optical pump-probe experiments[5–15] supported by theoretical investigations[16–21] the following picture of hot carrier dynamics in graphene has emerged. The matrix element describing the coupling between electrons and light is anisotropic with nodes along the direction of light polarization, resulting in a correspondingly anisotropic initial distribution of electrons and holes peaked at $E = \pm\hbar\omega_{pump}/2$ away from the Dirac point[19]. Subsequent carrier-carrier scattering leads to an ultrafast thermalization of the electronic system resulting in a hot Fermi-Dirac (FD) distribution with a momentum-dependent electronic temperature within some tens of femtoseconds[19]. This distribution cools down and becomes isotropic via the emission of optical phonons within $\sim$200 fs[5,6,19], resulting in a hot optical phonon population that has been directly observed with time-resolved Raman scattering[8,11,15]. These hot phonons subsequently decay into two acoustic modes on a picosecond time scale[8,11,13,15]. Furthermore, in the presence of lattice defects, the electronic system can couple directly to acoustic phonons resulting in supercollision cooling of the electronic system[21–23].

The initial ultrafast thermalization resulting in an anisotropic FD distribution is beyond the time resolution of most pump-probe experiments. Measurements performed with sub 10 fs pulse duration, however, indicate the existence of separate electron and hole distributions in the conduction and valence band at early times[7,14]. These findings have been confirmed by time-resolved photoemission experiments[24,25] and the observation of a transient negative optical conductivity[26]. In Ref.[17] the occurrence of population inversion after optical excitation has been attributed to the dominance of intraband electron-phonon scattering at early times. The decay of the population inversion on the femtosecond time scale is believed to be driven mainly by Auger recombination[17,25].

Recently, the prediction of carrier multiplication by impact ionization[18–20] has motivated considerable experimental activity, revealing crucial misconceptions and resulting in conflicting interpretations. We would like to clarify that the observation of hot-carrier multiplication in Refs.[27,28] is no proof for multiple electron-hole pair generation by a single absorbed photon as predicted by[18–20]. While Ref.[29], based on the comparison of the measured transmission change after optical excitation with different theoretical models, argues in favor of carrier multiplication, tr-ARPES experiments find no indication for this effect[25,30].

In the present work we show that scattering rates of photo-excited carriers in graphene measured with tr-ARPES indeed resemble the MDC line width determined by static ARPES as predicted by[4]. Furthermore, we find that the rise time of the number of carriers in the conduction band for excitation at 1.5 eV is slightly longer than the pump pulse duration. Before attributing this finding to the occurrence of carrier multiplication, alternative explanations for an increased rise time need to be excluded in a more systematic study.

2 Equilibrium properties of graphene

The present study is performed on quasi-freestanding hydrogen-intercalated graphene monolayers on a SiC(0001) substrate as first reported in Ref.[31]. The static

band structure perpendicular to the ΓK-direction is displayed in Fig. 1a. The samples are slightly hole-doped with the Dirac point about 200 meV above the Fermi level. The influence of many-body interactions in similar samples has been addressed previously in a high-resolution ARPES measurement[32]. Figure 1b shows the measured line width of momentum distribution curves (MDCs) as a function of energy. The steep increase in line width between the Fermi level and $E \approx -200$ meV is caused by the strong coupling of the electrons to the E_{2g} phonon mode at Γ and the A_1' phonon mode at K[16,32]. The continuous increase at lower energies is attributed to electron-hole scattering[32].

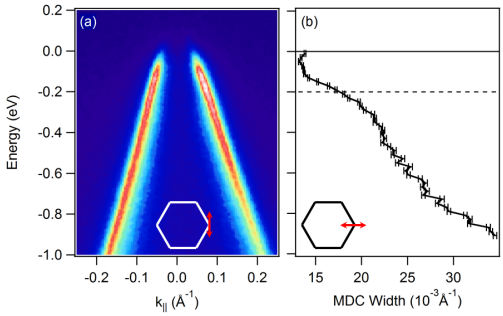

Fig. 1 (a) Static band structure of hydrogen-intercalated monolayer graphene around the K-point of the Brillouin zone measured along a cut perpendicular to the ΓK-direction (see inset). The samples are slightly hole-doped with the Dirac-point ~ 200 meV above the Fermi level. Panel (b) shows fit results of the Lorentzian line width for momentum distribution curves (MDCs) along the ΓK-direction (see inset) as a function of energy for a hydrogen-intercalated graphene monolayer. The horizontal dashed black line indicates the energy of the E_{2g} phonon mode.

3 Time- and angle-resolved photoemission spectroscopy

Photoemission spectroscopy is based on the photoelectric effect, where an incident photon in the extreme ultra-violet (EUV) range impinges on the surface of a crystal and releases a photoelectron. The resulting photocurrent as a function of kinetic energy and emission angle gives direct access to the electronic structure in momentum space. The photocurrent is directly proportional to the spectral function $A(\vec{k},E)$ of the sample that, using the sudden approximation, is given by[33]

$$A(\vec{k},E) = \frac{1}{\pi} \frac{Im\left(\Sigma(\vec{k},E)\right)}{\left[E - E^0_{\vec{k}} - Re\left(\Sigma(\vec{k},E)\right)\right]^2 + \left[Im\left(\Sigma(\vec{k},E)\right)\right]^2},$$

where $E^0_{\vec{k}}$ is the single particle dispersion and $\Sigma(\vec{k},E)$ is the complex self-energy due to many-body interactions. $A(\vec{k},E)$ is a Lorentzian function with the peak position at $E^0_{\vec{k}} + Re\left(\Sigma(\vec{k},E)\right)$ and a peak width of $Im\left(\Sigma(\vec{k},E)\right)$. Thus, ARPES

presents the ideal tool to investigate the influence of many-body interactions on the electronic structure. A careful analysis of peak positions and line widths has been used to identify many-body interactions in graphene[2,32]. More importantly, the imaginary part of the self-energy $Im\left(\Sigma(\vec{k},E)\right)$ can be obtained directly by transferring the technique to the time domain, where the energy- and momentum-dependent scattering rate is given by[4]

$$1/\tau\left(\vec{k},E\right) = -2Im\left(\Sigma(\vec{k},E)\right).$$

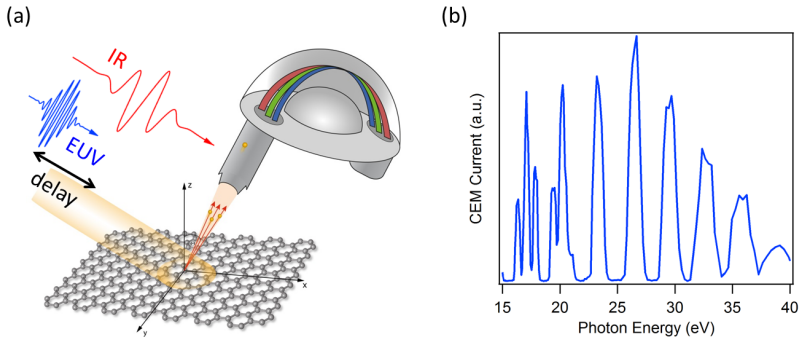

Fig. 2 (a) Schematic setup for time- and angle-resolved photoemission spectroscopy. The graphene samples are excited with femtosecond laser pulses at $\hbar\omega_{pump} = 1.5$ eV. The response of the electronic structure is probed with angle-resolved photoemission spectroscopy, where a time-delayed pulse at $\hbar\omega_{probe} \approx 30$ eV ejects photoelectrons from the sample. Both the emission angle and the kinetic energy of the photoelectrons are measured with a hemispherical analyzer, giving direct access to the distribution of electrons in momentum space as a function of energy and pump-probe delay. (b) Typical EUV spectrum from high harmonics generation in argon.

A schematic setup for tr-ARPES is shown in Fig. 2a. A pump pulse at $\hbar\omega_{pump}$ excites the sample and the response of the electronic structure is probed with ARPES, where a time-delayed EUV pulse releases photoelectrons. For the present experiment the pump wavelength was chosen to be $\hbar\omega_{pump} = 1.5$ eV, the fundamental wavelength of a femtosecond Ti:Sapphire laser system (800 nm, 60 fs, 1 kHz). For the EUV probe we use high harmonics of the fundamental wavelength generated in an argon plasma. A typical EUV spectrum obtained by high harmonics generation in argon is shown in Fig. 2b. The spectrum covers the energy range between 15 and 40 eV. A time-preserving grating monochromator[34] is used to select a single harmonic at $\hbar\omega_{probe} \approx 30$ eV for the present graphene measurements.

Figure 3 shows snapshots of the electronic structure of a quasi-freestanding graphene monolayer in the vicinity of the K-point for different time delays after excitation at $\hbar\omega_{pump} = 1.5$ eV (upper panel) together with the corresponding pump-probe signal (lower panel). The pump-probe signal is dominated by an instantaneous heating of the electronic system accompanied by a momentum-broadening of the π-band and subsequent relaxation within ~ 1 ps. Figure 3 also

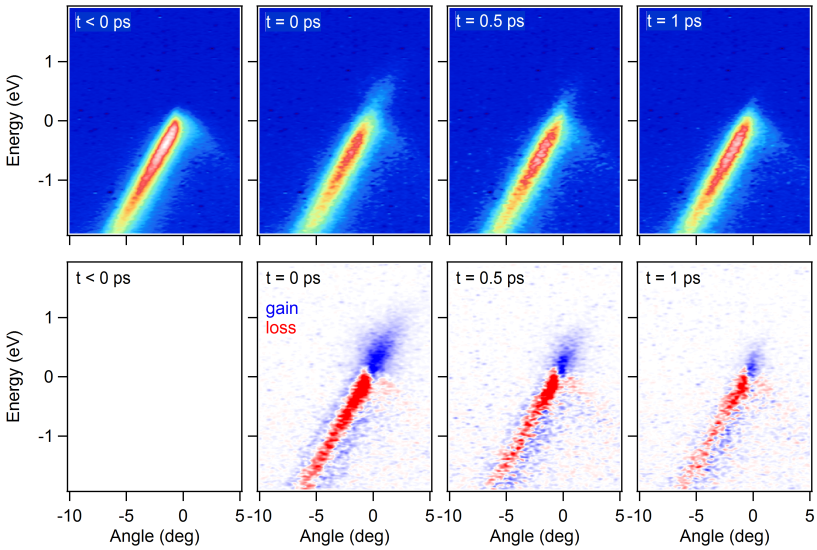

Fig. 3 Upper panel: Snapshots of the band structure along the ΓK-direction for a hydrogen-intercalated graphene monolayer for different pump-probe delays for excitation at $\hbar\omega_{pump} = 1.5$ eV. Lower panel: corresponding pump-probe signal.

illustrates the main advantage of tr-ARPES over all-optical pump-probe techniques: tr-ARPES can track the whereabouts of each electron as a function of energy, momentum and time, delivering a complete set of information about non-equilibrium carrier dynamics. Therefore, tr-ARPES is the technique of choice to address the existing controversies concerning carrier multiplication in graphene.

The instantaneous heating and subsequent cooling of the electronic system after excitation at $\hbar\omega_{pump} = 1.5$ eV is addressed in Fig. 4, where we plot the width of the Fermi cut-off (obtained by fitting momentum-integrated energy distribution curves in the vicinity of the Fermi level with a FD distribution) as a function of delay. We want to point out that, for the present excitation regime, the occupancy of the bands can be described by a single FD distribution at all times, indicating very rapid thermalization of the electronic system. The data points in Fig. 4 have been fitted with an error function accounting for the rise time of the signal and two exponential decays. The two decay times, $\tau_1 = 207 \pm 25$ fs and $\tau_2 = 1.5 \pm 0.2$ ps, are commonly attributed to the emission of optical and acoustic phonons, respectively. Our results agree well with values published in literature[5–21] and support the established picture of hot carrier relaxation in graphene.

4 Self-energy from tr-ARPES

According to Ref.[4] non-equilibrium dynamics for a model photo-excited electron-phonon system measured with tr-ARPES are determined by the static self-energy alone. The phonon energy ω_{ph} is found to determine the size of an energy window around the Fermi level, where a long-lived pump-probe signal is ex-

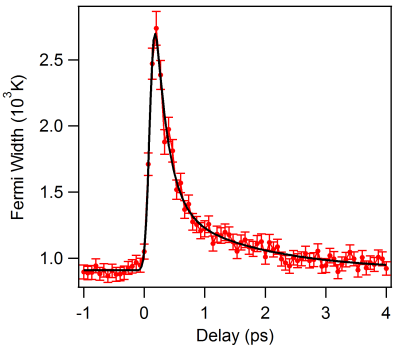

Fig. 4 $\hbar\omega_{pump} = 1.5$ eV. Width of the Fermi level (data points) as a function of pump-probe delay obtained by fitting momentum-integrated energy distribution curves in the vicinity of the Fermi level with a Fermi-Dirac function. The continuous line represents a double exponential fit with $\tau_1 = 207 \pm 25$ fs typically attributed to electron - optical phonon scattering and $\tau_2 = 1.5 \pm 0.2$ ps due to emission of acoustic phonons.

pected. Electrons will decay rapidly for $|E| > \omega_{ph}$, while for $|E| < \omega_{ph}$ decay via phonon emission is no longer possible. Following Ref.[4] we plot the momentum-integrated pump-probe signal as a function of delay (Fig. 5b) and determine the energy-dependence of the scattering time from our tr-ARPES data (Fig. 5c). Finally, we compare our results to the MDC line width obtained from static ARPES measurements on a similar sample (Fig. 6).

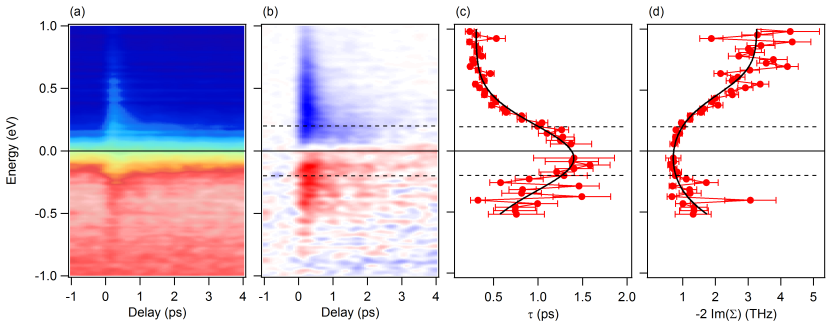

Fig. 5 (a) Momentum-integrated photocurrent as a function of pump-probe delay for excitation at $\hbar\omega_{pump} = 1.5$ eV. (b) Corresponding pump-probe signal. (c) Relaxation time τ as a function of energy obtained by fitting pump-probe time traces at different energies with an exponentially decaying function. (d) Inverse lifetime $1/\tau = -2\mathrm{Im}(\Sigma)$ as a function of energy. Continuous black lines are guides to the eye. Horizontal dashed black lines indicate the energy of the in-plane bond-stretching phonon mode.

The data analysis is done as follows: in a first step, the snapshots in Fig. 3 are integrated over momentum and plotted as a function of delay (Fig. 5a). From the momentum-integrated data we subtract the photocurrent at negative time delays to obtain Fig. 5b. Then we extract time traces at constant energy and fit them with an exponentially decaying function resulting in the scattering times plotted in Fig. 5c. In Fig. 5d we plot the scattering rate $1/\tau$ that is directly proportional

to the imaginary part of the self-energy[4].

In Figs. 5b, c, and d dashed black lines mark the size of the phonon window discussed above. As predicted,[4] decay times are much longer inside than outside of this phonon window. Hence, plots similar to the one in Fig. 5b offer a direct way to visualize the existence of relaxation bottlenecks in photo-excited systems associated with the coupling to a bosonic mode.

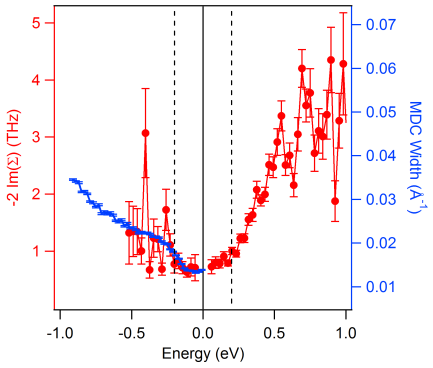

Fig. 6 Direct comparison between MDC width from Fig. 1c and $1/\tau$ from Fig. 5d. Vertical dashed black lines indicate the energy of the in-plane bond-stretching phonon mode.

Both the scattering rate from tr-ARPES data and the MDC line width from static ARPES data are proportional to the imaginary part of the self-energy. In Fig. 6 we directly compare the two quantities to find out whether the non-equilibrium dynamics after photo-excitation are completely determined by the static self-energy as predicted in Ref.[4]. We indeed find that, within the experimental error bars, the scattering rate and the MDC line width follow the same trend for $E < 0$. In this context tr-ARPES results nicely complement the information gained by static ARPES investigations, as tr-ARPES directly measures the imaginary part of the self-energy via $1/\tau = -2Im(\Sigma)$ both below and above the equilibrium chemical potential.

5 Carrier multiplication

It has been proposed that, in graphene, the absorption of a single photon may generate several electron-hole pairs via impact ionization[18–20]. This process is illustrated in Fig. 7a. The prediction of carrier multiplication is based on the assumption that an ultrashort pump pulse generates a non-thermal carrier distribution with a narrow distribution of electrons in the conduction band and holes in the valence band centered at $E_D \pm \hbar\omega_{pump}/2$. Such a carrier distribution offers a large phase space for impact ionization (green arrows in Fig. 7) where part of the excess energy of a photo-excited electron is used to generate a second electron-hole pair. The inverse process of Auger heating is suppressed by Pauli blocking. According to Refs.[18–20] carrier multiplication is expected to be robust even in the presence of electron-phonon coupling, where energy rapidly dissipates to the phonon bath. Optimum experimental conditions for the observation of carrier

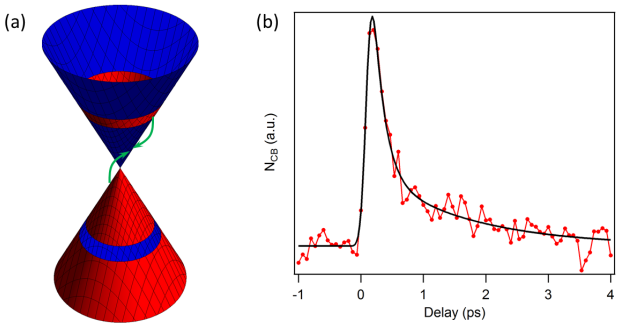

Fig. 7 (a) Schematic of carrier multiplication via impact ionization for the given non-equilibrium carrier distribution. Occupied (empty) states are shown in red (blue). (b) Number of carriers in the conduction band N_{CB} as a function of delay (data points) together with fit (continuous line).

multiplication are a small pump fluence, a high excitation energy, a low initial temperature, and charge neutral graphene[20,25].

In Ref.[29] the authors have modeled experimental transmission changes at $\hbar\omega_{pump} = 2.25$ eV and $\hbar\omega_{probe} = 1.37$ eV, incorporating either dynamical screening that suppresses Auger scattering or static/regularized dynamical screening with a high impact of Auger scattering. The latter seems to result in a good agreement with the experimental data. The extracted carrier multiplication factor reaches a maximum value of ~ 1.1. Recent tr-ARPES results[25,30] using $\hbar\omega_{pump} = 950$ meV did not find any indication for carrier multiplication. In principle, tr-ARPES is the tool of choice for the search for carrier multiplication as it directly measures the number of electrons in the conduction band as a function of energy, momentum and time. However, the excitation energy for the tr-ARPES experiments is lower than the one in Ref.[29], so that carrier multiplication may occur in Ref.[29] but not in Refs.[25,30]. Clearly, the possible occurrence of carrier multiplication in graphene deserves further attention.

In Fig. 5b we plot the momentum-integrated pump-probe signal for excitation at $\hbar\omega_{pump} = 1.5$ eV as a function of delay. This graph directly mirrors the transient changes of the electron distribution across the Dirac cone along the ΓK-direction. The smoking gun evidence for the occurrence of carrier multiplication would be that the number of electron-hole pairs keeps increasing after the pump pulse is already gone[18]. In order to determine the number of carriers in the conduction band N_{CB} along ΓK, we integrate the data in Fig. 5b for $E > E_D = 200$ meV (data points in Fig. 7b). The data are fitted with an error function to describe the rise time and two exponential decays (continuous line in Fig. 5b). We find a rise time of 100 ± 10 fs that is slightly longer than the measured pulse duration of 60 fs.

This finding may be interpreted in terms of carrier multiplication. However, this is not the only possible explanation. As discussed in the introduction, interband transitions result in an anisotropic carrier distribution at earliest times with nodes along the direction of the pump polarization[19]. The pump polarization in the present experiment is along the ΓK-direction, i.e., the transient band struc-

ture is measured along a node of the initially anisotropic carrier distribution. This means that carriers in the conduction band can be detected only after the initially anisotropic distribution has partially relaxed via phonon emission. Therefore, the increased rise time may also originate from the transition from an anisotropic to an isotropic distribution of carriers on the 200 fs time scale of electron-phonon coupling. Further, we want to point out that for the present excitation regime we observe a thermal FD distribution of carriers at all times (see Fig. 4) which is not expected to result in carrier multiplication[25].

To conclude, a definite proof of carrier multiplication in graphene by tr-ARPES needs to be based on a complete mapping of the whole Dirac cone. A single cut along any particular direction in momentum space is not sufficient to exclude the contribution of an initially anisotropic carrier distribution to an increased rise time. Furthermore, an observation of carrier multiplication might require sub 10 fs time resolution to enable access to the initially non-thermal carrier distribution that lies at the heart of carrier multiplication.

Summary and outlook

In summary, we have used tr-ARPES to determine the imaginary part of the self-energy $Im(\Sigma)$ in graphene by measuring the scattering rate $1/\tau = -2Im(\Sigma)$ as a function of energy after photo-excitation at $\hbar\omega_{pump} = 1.5$ eV. A comparison with static MDC line widths indicates that the dynamics of photo-excited carriers in graphene are determined by the equilibrium self-energy as suggested in Ref.[4]. Furthermore, we have addressed the issue of carrier multiplication in graphene. While a definite proof for its existence is still missing, we have identified important steps towards a future, more systematic study of carrier multiplication in graphene using tr-ARPES.

Acknowledgments

We thank Haiyun Liu and Hubertus Bromberger for technical support with the tr-ARPES measurements and Matteo Mitrano for fruitful discussions and comments concerning the present manuscript. Stiven Forti, Camilla Coletti and Konstantin V. Emtsev helped with the static ARPES measurements, partially supported by the German Research Foundation (DFG) within the priority program 'graphene' SPP 1459 (Sta 315/8-1).

References

1 P. R. Wallace, *Phys. Rev.* **71**, 622 (1947)
2 A. Bostwick, T. Ohta, T. Seyller, K. Horn, and E. Rotenberg, *Nat. Phys.* **3**, 36 (2007)
3 A. Bostwick, F. Speck, T. Seyller, K. Horn, M. Polini, R. Asgari, A. H. MacDonald, and E. Rotenberg, *Science* **328**, 999 (2010)
4 M. Sentef, A. F. Kemper, B. Moritz, J. K. Freericks, Z.-X. Shen, and T. P. Devereaux, *Phys. Rev. X* **3**, 041033 (2013)
5 T. Kampfrath, L. Perfetti, F. Schapper, C. Frischkorn, and M. Wolf, *Phys. Rev. Lett.* **95**, 187403 (2005)
6 S. Butscher, F. Milde, M. Hirtschulz, E. Malić, and A. Knorr, *Appl. Phys. Lett.* **91**, 203103 (2007)
7 M. Breusing, C. Ropers, and T. Elsaesser, *Phys. Rev. Lett.* **102**, 086809 (2009)

8 H. Yan, D. Song, K. F. Mak, I. Chatzakis, J. Maultzsch, and T. F. Heinz, *Phys. Rev. B* **80**, 121403(R) (2009)

9 H. Wang, J. H. Strait, P. A. George, S. Shivaraman, V. B. Shields, M. Chandrashekhar, J. Hwang, F. Rana, M. G. Spencer, C. S. Ruiz-Vargas, and J. Park, *Appl. Phys. Lett.* **96**, 081917 (2010)

10 D. Sun, C. Divin, C. Berger, W. A. de Heer, P. N. First, and T. B. Norris, *Phys. Rev. Lett.* **104**, 136802 (2010)

11 K. Kang, D. Abdula, D. G. Cahill, and M. Shim, *Phys. Rev. B* **81**, 165405 (2010)

12 C. H. Lui, K. F. Mak, J. Shan, and T. F. Heinz, *Phys. Rev. Lett.* **105**, 127404 (2010)

13 P. J. Hale, S. M. Hornett, J. Moger, D. W. Horsell, and E. Hendry, *Phys. Rev. B* **83**, 121404(R) (2011)

14 M. Breusing, S. Kuehn, T. Winzer, E. Malić, F. Milde, N. Severin, J. P. Rabe, C. Ropers, A. Knorr, and T. Elsaesser, *Phys. Rev. B* **83**, 153410 (2011)

15 I. Chatzakis, H. Yan, D. Song, S. Berciaud, and T. F. Heinz, *Phys. Rev. B* **83**, 205411 (2011)

16 N. Bonini, M. Lazzeri, N. Marzari, and F. Mauri, *Phys. Rev. Lett.* **99**, 176802 (2007)

17 T. Winzer, E. Malić, and A. Knorr, *Phys. Rev. B* **87**, 165413 (2013)

18 T. Winzer, A. Knorr, and E. Malić, *Nano Lett.* **10**, 4839 (2010)

19 E. Malić, T. Winzer, E. Bobkin, and A. Knorr, *Phys. Rev. B* **84**, 205406 (2011)

20 T. Winzer, and E. Malić, *Phys. Rev. B* **85**, 241404(R) (2012)

21 J. C. W. Song, M. Y. Reizer, and L. S. Levitov, *Phys. Rev. Lett.* **109**, 106602 (2012)

22 A. C. Betz, S. H. Jhang, E. Pallecchi, R. Ferreira, G. Fève, J-M. Berroir, and B. Plaçais, *Nat. Phys.* **9**, 109 (2013)

23 M. W. Graham, S.-F. Shi, D. C. Ralph, J. Park, and P. L. McEuen, *Nat. Phys.* **9**, 103 (2013)

24 S. Gilbertson, T. Durakiewicz, J.-X. Zhu, A. D. Mohite, A. Dattelbaum, and G. Rodriguez, *J. Vac. Sci. Technol. B* **30**, 03D116 (2012)

25 I. Gierz, J. C. Petersen, M. Mitrano, C. Cacho, I. C. E. Turcu, E. Springate, A. Stöhr, A. Köhler, U. Starke, and A. Cavalleri, *Nat. Mater.* **12**, 1119 (2013)

26 T. Li, L. Luo, M. Hupalo, J. Zhang, M. C. Tringides, J. Schmalian, and J. Wang, *Phys. Rev. Lett.* **108**, 167401 (2012)

27 K. J. Tielrooij, J. C. W. Song, S. A. Jensen, A. Centeno, A. Pesquera, A. Zurutuza Elorza, M. Bonn, L. S. Levitov, and F. H. L. Koppens, *Nat. Phys.* **9**, 248 (2013)

28 Justin C. W. Song, Klaas J. Tielrooij, Frank H. L. Koppens, and Leonid S. Levitov, *Phys. Rev. B* **87**, 155429 (2013)

29 D. Brida, A. Tomadin, C. Manzoni, Y.J. Kim, A. Lombardo, S. Milana, R.R. Nair, K.S. Novoselov, A.C. Ferrari, G. Cerullo, and M. Polini, *Nat. Commun.*, DOI: 10.1038/ncomms2987 (2013)

30 J. C. Johannsen, S. Ulstrup, F. Cilento, A. Crepaldi, M. Zacchigna, C. Cacho, I. C. E. Turcu, E. Springate, F. Fromm, C. Raidel, T. Seyller, F. Parmigiani, M. Grioni, and P. Hofmann, *Phys. Rev. Lett.* **111**, 027403 (2013)

31 C. Riedl, C. Coletti, T. Iwasaki, A. A. Zakharov, and U. Starke, *Phys. Rev. Lett.* **103**, 246804 (2009)

32 S. Forti, K. V. Emtsev, C. Coletti, A. A. Zakharov, C. Riedl, and U. Starke, *Phys. Rev. B* **84**, 125449 (2011)

33 S. Hüfner, "Photoelectron Spectroscopy, Principles and Applications," ISBN 978-3-662-09280-4

34 F. Frassetto, C. Cacho, C. A. Froud, I. C. E. Turcu, P. Villoresi, W. A. Bryan, E. Springate, and L. Poletto, *Opt. Express* **19**, 19169 (2011)

